Modeling of CO_2 Capture by Aqueous Monoethanolamine

Stefano Freguia and Gary T. Rochelle
Dept. of Chemical Engineering, The University of Texas at Austin, Austin, TX 78712

The process for CO_2 removal from flue gases was modeled with RateFrac. It consists of an absorber, a stripper, and a cross heat exchanger. The solvent used in the model contains about 30 wt % monoethanolamine (MEA) in water. MEA reacts with CO_2 in the packed absorber. The finite reaction rate requires a kinetic characterization. The RateFrac absorber model was integrated with a FORTRAN user kinetic subroutine to make the model consistent with the interface pseudo-first-order model and with a regressed Electrolyte-NRTL equilibrium model. It was adjusted with laboratory wetted wall column data and field data from a commercial plant. Sensitivity analyses were performed on process variables to find operating conditions at low steam requirement. Many variables strongly affect the process performance, but an overall optimization shows that there are no economical ways to reduce the steam requirements by more than 10%. The reboiler duty can be reduced from that of a base case representing current industrial operating conditions, by 5% if acids are added to the solvent, by 10% if the absorber height is increased by 20%, and by 4% if the absorber is intercooled with a duty of one-third of the reboiler duty. The power plant lost work is affected by varying stripper pressure, but not significantly, so any convenient pressure can be chosen to operate the stripper.

Introduction

The removal and sequestration of CO_2 from combustion gases is an important technological alternative to address global climate change. Absorption/stripping with aqueous monoethanolamine (MEA) has been commercially applied in small plants for CO_2 recovery. Aqueous MEA is an effective solvent for CO_2 capture, but a system for 90% CO_2 removal can reduce the efficiency of a power plant from 40% to 30% (IEA Greenhouse R&D Programme, 2002).

The absorption/stripping process is shown in Figure 1. Flue gas contacts the aqueous solvent at 1 atm and 40–60°C, in a countercurrent, packed absorber. Typical sources of flue gas include gas-fired turbines, giving 3 mol % CO_2 and coal-fired plants, giving 10–12% CO_2.

One version of this process uses approximately 30 wt % MEA; another uses 15–20 wt % MEA (Liljedahl et al., 2001). Typically the lean solvent has a CO_2 loading of 0.1–0.2 mol/mol MEA, and the rich solvent has a loading of 0.4–0.5.

Correspondence concerning this article should be addressed to G. Rochelle.

The rich solvent is stripped by steam in a countercurrent, reboiled column at 1.5–2 atm and 100–120°C to produce pure CO_2. Heat is recovered from the hot lean solvent by cross-exchange with cold rich solvent. The lean solvent is typically cooled further to approximately 40°C.

Integrated models for this process have been created; they either use commercial software or language codes. TSWEET has been used since the early 1980s for modeling of acid gas removal (Holmes et al., 1984). Another software package in use is AMSIM, which uses a rigorous nonequilibrium-stage model (Zhang et al., 1996). Weiland and Dingman (2001) developed a program called ProTreat for the rate-based simulation of columns. Along with commercial packages, programs written in Fortran or Visual Basic have been developed. These programs have the advantage of being specific for amine gas treating. A model by Al-Baghli et al. (2001) uses this method. This approach is usually slower, and presents challenges in simulating the whole process.

The purpose of this work is to understand how the design variables affect each other at the level of the whole process,

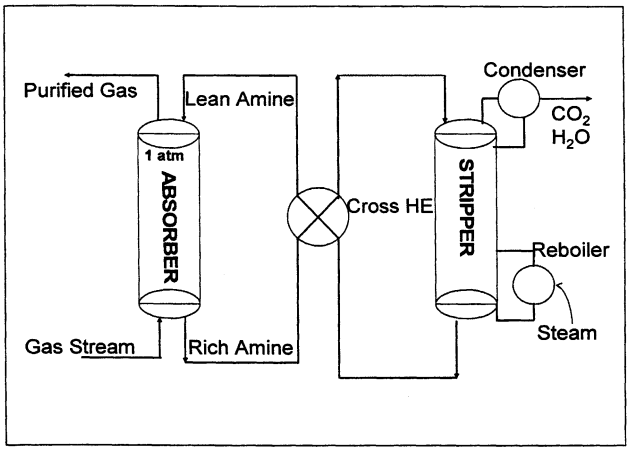

Figure 1. Absorption/stripping process for CO_2 removal with alkanolamines.

not of the single absorber and stripper. Aspen Plus was found to be suitable for this type of analysis, and it was chosen as a framework for the model built in this work. The model was built to analyze the effect on energy requirements of several process variables. The goal was to find operating conditions that allow CO_2 removal with less energy.

Model Development

The absorber and stripper were both modeled with RateFrac, a rate-based model framework in Aspen Plus. In the absorber, the reactions involving CO_2 were described with a kinetic model. In the stripper all the reactions were set to equilibrium, due to the higher operating temperature. This approach required that a rigorous thermodynamic model and a rigorous rate model be implemented in Aspen Plus.

Thermodynamic model

The thermodynamics were described with the Electrolyte-NRTL framework, developed by Chen et al. (1979), and modified by Mock et al. (1986) for mixed-solvent systems. The model reproduces the one developed by Austgen (1989), with some interaction parameters regressed in order to match the data of Jou et al. (1995), considered more accurate than those of Lee et al. (1976) and others, used by Austgen. The reactions incorporated in the model are the same as those included by Austgen (1989). The values of the constants and the interaction parameters can be found in Freguia (2002)

$$MEACOO^- + H_2O \overset{K_{carb}}{\longleftrightarrow} MEA + HCO_3^- \quad (1a)$$

$$CO_2 + 2H_2O \overset{K_{a,CO_2}}{\longleftrightarrow} HCO_3^- + H_3O^+ \quad (1b)$$

$$HCO_3^- + H_2O \overset{K_{a,HCO_3^-}}{\longleftrightarrow} CO_3^{--} + H_3O^+ \quad (1c)$$

$$MEAH^+ + H_2O \overset{K_{a,MEAH^+}}{\longleftrightarrow} MEA + H_3O^+ \quad (1d)$$

$$2H_2O \overset{K_w}{\longleftrightarrow} H_3O^+ + OH^- \quad (1e)$$

In addition to the species included in the Austgen framework, this model also included heat stable salts (HSS) modeled as formates, formed according to the irreversible reaction

$$MEA + HCOOH \rightarrow MEAH^+ HCOO^- \quad (2)$$

HSS are normally present in absorption/stripping processes for acid gas removal. They are products of MEA neutralization with strong acids. Typical forms of HSS are sulfates or formates. The HSS were modeled in Aspen Plus by including formate as a component and assigning to it the same interaction parameters as $MEACOO^-$. No VLE data were available with formate in the system. The important property of the $HCOO^-$ anion is its charge. This extra charge has to be balanced by $MEAH^+$, thus making some of the MEA less available for CO_2 absorption. The presence of HSS alters the equilibrium, increasing $P^*_{CO_2}$ at a given loading, which is redefined according to Eq. 3. This fact causes the absorber driving forces to be reduced, and the driving forces in the stripper to be increased

$$CO_s \text{ Loading} = \alpha = \frac{[CO_2]_{tot}}{[MEA]_{tot} - [HSS]} = \frac{[CO_2]_{tot}}{[MEA]_{free}} \quad (3)$$

The concentration of HSS is also given by the loading

$$\text{HSS loading} = \frac{[HSS]}{[MEA]_{tot}} \quad (4)$$

Rate model

The rate model used in the absorber was made consistent with the Electrolyte-NRTL thermodynamic model and with the interface-pseudo-first-order (IPFO) approximate model for mass transfer, through a Fortran kinetic subroutine for RateFrac. In the rate model the reactions were the same as in the equilibrium model, except reactions 1a and 1b, which were replaced by kinetic reversible reactions 5a and 5b. The direct reactions were given second-order rate expressions, given by Eqs. 6 and 7

$$CO_2 + MEA + H_2O \xrightarrow{K_{2,MEA}} MEACOO^- + H_3O^+ \quad (5a)$$

$$CO_2 + OH^- \xrightarrow{K_{2,OH^-}} HCO_3^- \quad (5b)$$

$$R_{CO_2-MEA} = k_{2,MEA} C^2_{tot} x_{MEA} a_{CO_2} \quad (6)$$

$$R_{CO_2-OH^-} = k_{2,OH^-} C^2_{tot} x_{OH^-} a_{CO_2} \quad (7)$$

Reaction 5b is almost always negligible in the reaction boundary layer, but it is necessary to provide a route for the reversible production of bicarbonate.

The IPFO model assumes that a consequence of the fast reaction kinetics of CO_2 is that the concentration of every other species in solution is constant at its interface value. This assumption has the advantage that the CO_2 flux can be calculated analytically, using Eq. 8, where the driving force is expressed in terms of activities, calculated using the Elec-

trolyte-NRTL model

$$N_{CO_2} = \sqrt{\left(k_{2,MEA}[MEA]_i + k_{2,OH^-}[OH^-]_i\right)\frac{D_{CO_2}}{\gamma_{CO_2}}} \times \left(a_{CO_2,i} - a^*_{CO_2,i}\right) \quad (8)$$

The term $a^*_{CO_2}$ is defined by Eq. 9

$$a^*_{CO_2,i} = \frac{\frac{k_{2,MEA}}{K_{CO_2-MEA}}\frac{a_{MEACOO^-}a_{H_3O^+}}{a_{H_2O}\gamma_{MEA}} + \frac{k_{2,OH^-}}{K_{CO_2-OH^-}}\frac{a_{HCO_3^-}}{\gamma_{OH^-}}}{k_{2,MEA}x_{MEA} + k_{2,OH^-}x_{OH^-}} \quad (9)$$

In the equation the rates of reverse reactions 5a and 5b were calculated using their equilibrium constants. Equation 9 is an arbitrary allocation of the production rate of CO_2 between reactions 5a and 5b.

Equation 10 defines the rate constant used for reaction 5a. The temperature dependence is derived from wetted wall column data from Dang (2001). The constant A was adjusted to match commercial plant data, provided by Fluor Daniel, Inc. Equation 10 with Dang's data implies rate constants higher than the values measured by Hikita et al. (1977) by factors of 2 to 5 at 40–60°C. This difference is significant, and it can be attributed to the increased solution ionic strength in loaded solutions. This is consistent with the results of Pinsent et al. (1956), who showed that ionic strength as 1 M NaCl increased the reaction rate of CO_2 with ammonia by a factor of 3

$$\ln k_{2,MEA} = A - \frac{904.6}{T} \quad (10)$$

Equation 11 gives the expression for the rate constant of reaction 5b, from Sherwood et al. (1975)

$$\ln k_{OH^-} = 31.396 - \frac{6658}{T} \quad (11)$$

The diffusivity of CO_2 was calculated using the Stokes–Einstein relationship proposed by Pacheco (1998), given by Eq. 12

$$D_{CO_2} = D_{CO_2,water}\left(\frac{\mu_{water}}{\mu_{solution}}\right)^{0.545} \quad (12)$$

The viscosity of the solution and that of water were calculated using the expression developed by Weiland (1996), which accounts for temperature, MEA concentration, and CO_2 loading. The addition of MEA to water increases the viscosity, thus reducing the diffusivity.

The activity coefficient of CO_2 (γ_{CO_2}) serves to transform the concentration-based diffusivity into an activity-based diffusivity. It is calculated by the Electrolyte-NRTL model.

Other RateFrac methods

The RateFrac module of Aspen Plus was used to integrate the heat transfer and multicomponent mass-transfer relationships for a packed absorber and stripper. Among the many rate phenomena included, the most important were CO_2 liquid film mass transfer, H_2O gas film mass transfer, and gas film heat transfer. This model used the rigorous Electrolyte-NRTL thermodynamics to predict enthalpies, equilibrium vapor pressures of CO_2 and H_2O, and solution speciation. Gas-film and liquid-film mass- and heat-transfer coefficients were obtained as a function of liquid and gas flow rates and properties with the default correlations of RateFrac.

Model validation

The rate and equilibrium model were used to simulate a base case for the absorption/stripping process. The base case was developed on proprietary data from a commercial plant. CO_2 loading, packing height, and stream flow rates will not be disclosed here. The reboiler duties are normalized to the moles of CO_2 removed and they are divided by a typical operating value.

The constant A in Eq. 10 was adjusted in order to match the base-case removal. Table 1 compares the plant data with the model results, for the base case and three other test runs.

In the base-case simulation CO_2 removal is well matched; the reboiler duty is overpredicted by 3.5%. In the other three runs the main mismatch is in the reboiler duty, which is overpredicted by 10 to 30%; the CO_2 removal is underpredicted by up to 4%.

Effect of Process Variables on Energy Requirements

Model methods and base-case conditions

The following conditions were used in the base case, and were kept at those values in all the runs, unless otherwise stated.

- MEA concentration, $[MEA]_{tot}$: 33.5 wt %
- HSS loading: 0.1 mol/mol MEA_{tot}
- Stripper bottom pressure: 1.7 atm
- Absorber-solvent inlet temperature: 40°C

Table 1. Summary of Results of Model Validation with Commercial Plant Data

	Base Case	Model	Test 1	Model	Test 2	Model	Test 3	Model
Feed CO_2 (%)	3.13		2.87		3		2.86	
Vent CO_2 (%)	0.49	0.49	0.34	0.342	0.56	0.63	0.3	0.38
CO_2 recovery (%)	85.0	85.0	88.0	87.9	81.5	78.6	89.7	85.5
MEA (wt %)	30		28.2		26.6		29	
Relative Q_r	0.99	1.035	1.125	1.515	1.02	1.2	0.995	1.135

Table 2a. Detailed Simulation Results

Solvent Rate: 3% CO_2, 85% Removal, 33.5 wt. % MEA_{tot}, HSS Loading = 0.1, $P_{reboiler}$ = 1.77 atm, $Z_{absorber}/Z_{base\ case}$ = 1, $Z_{stripper}/Z_{base\ case}$ = 1

L/G_{mass}	Lean Loading	Rich Loading	Q_{rel}
0.633	0.11	0.417	1.490
0.684	0.13	0.415	1.269
0.735	0.15	0.413	1.145
0.780	0.16	0.411	1.085
0.863	0.18	0.408	1.050
0.912	0.19	0.406	1.053
0.968	0.20	0.404	1.063
1.032	0.21	0.402	1.078
1.299	0.24	0.393	1.143
1.775	0.27	0.383	1.255

Table 2b. Detailed Simulation Results *(continued)*

Absorber H: 33.5 wt. % MEA_{tot}, $Z_{stripper}/Z_{base\ case}$ = 1, HSS Loading = 0.1, $P_{reboiler}$ = 1.77 atm, Optimum L/G

CO_2 in Flue Gas (mol %)	CO_2 Removal (%)	$Z_{absorber}/Z_{base\ case}$	L/G_{mass}	Lean Loading	Rich Loading	Q_{rel}
3	85	0.6	3.29	0.26	0.321	1.87
3	85	1.6	0.82	0.20	0.440	0.95
3	90	0.8	3.37	0.28	0.343	1.69
3	90	1.0	1.18	0.19	0.368	1.25
3	90	1.6	0.85	0.19	0.435	0.97
10	90	0.8	5.42	0.29	0.417	1.11
10	90	1.0	2.68	0.19	0.442	0.96
10	90	1.6	2.61	0.20	0.460	0.90

Table 2c. Detailed Simulation Results *(continued)*

Stripper H: 3% CO_2, 85% Removal, 33.5 wt. % MEA_{tot}, $Z_{absorber}Z/_{base\ case}$ = 1, HSS Loading = 0.1, $P_{reboiler}$ = 1.77 atm, Optimum L/G

$Z_{stripper}/Z_{base\ case}$	L/G_{mass}	Lean Loading	Rich Loading	Q_{rel}
0.285	1.174	0.23	0.399	1.142
0.428	1.031	0.21	0.402	1.110
0.714	0.967	0.20	0.404	1.079

- Flue-gas water-saturation temperature: 115°C
- Flue-gas absorber-inlet temperature: 63°C
- Cross-exchanger hot-end temperature approach to equilibrium: 11°C

The cross heat exchanger was modeled in Aspen Plus with two separate HEATERS, connected by CALCULATOR blocks in such a way that the temperature approach of the hot end is fixed at 11°C and the heat duties of the two heaters are matched.

In the absorber the packing is modeled with 20 RateFrac segments; in the stripper 19 segments represent the packing, the bottom segment being the equilibrium reboiler. Some calculations were performed with 30 RateFrac segments representing the same total height of packing. There was less than 1% difference in the calculated reboiler duty. The top segment models a water wash. The rich feed enters the column "above" the second segment from the top. A condenser is modeled with a constant temperature (50°C) HEATER, and the reflux is fed above segment 1.

The solvent loop was not closed. It was kept open at the absorber inlet. In this way the lean solvent becomes an input to the model. Temperature, MEA concentration, and CO_2 loading of the stream are specified. The lean solvent rate is calculated with a design specification on the absorber block that keeps the removal at a specified value.

Sensitivity analyses were done on solvent rate, column heights, CO_2 removal, HSS loading, stripper pressure, and absorber temperature. The results of most runs are summarized in Table 2.

Table 2d. Detailed Simulation Results *(continued)*

Heat Stable Salts, MEA_{tot}: 3% CO_2, 85% Removal, $Z_{absorber}/Z_{base\ case}$ = 1, $Z_{stripper}/Z_{base\ case}$ = 1, $P_{reboiler}$ = 1.77 atm, Optimum L/G

MEA_{tot} (wt%)	HSS Loading	L/G_{mass}	Lean Loading	Rich Loading	Q_{rel}
20	0	1.25	0.22	0.451	1.201
20	0.05	1.279	0.21	0.448	1.197
20	0.10	1.321	0.20	0.444	1.196
20	0.15	1.314	0.18	0.441	1.195
20	0.20	1.319	0.16	0.437	1.198
20	0.25	1.39	0.15	0.432	1.203
30	0	0.97	0.23	0.431	1.093
30	0.05	0.951	0.21	0.427	1.084
30	0.10	0.99	0.2	0.421	1.074
30	0.15	0.988	0.18	0.416	1.067
30	0.20	0.996	0.16	0.41	1.063
30	0.25	1.021	0.14	0.402	1.066
36	0	0.928	0.23	0.407	1.087
36	0.05	0.86	0.2	0.402	1.069
36	0.10	0.896	0.19	0.396	1.053
36	0.15	0.951	0.18	0.387	1.043
36	0.20	0.871	0.14	0.381	1.04
36	0.25	0.894	0.12	0.372	1.033

Table 2e. Detailed Simulation Results *(continued)*

Stripper P: 3% CO_2, 85% Removal, 33.5 wt. % MEA_{tot}, HSS Loading = 0.1, $Z_{absorber}/Z_{base\ case}$ = 1, $Z_{stripper}/Z_{base\ case}$ = 1, Optimum L/G

$P_{reboiler}$	$D_{stripper}/D_{base\ case}$	L/G_{mass}	Lean Loading	Rich Loading	Q_{rel}	Relative Lost Work
0.5	1.529	1.93	0.28	0.384	2.102	0.322
2.04	0.824	0.81	0.17	0.411	1.019	0.243
2.43	0.824	0.78	0.16	0.413	0.974	0.24
3.06	0.765	0.71	0.14	0.415	0.928	0.241
3.40	0.765	0.68	0.13	0.416	0.909	0.243
3.74	0.765	0.66	0.12	0.417	0.892	0.244

Table 2f. Detailed Simulation Results *(continued)*

Absorber Intercooling: 3% CO_2, 85% Removal, 33.5 wt. % MEA_{tot}, HSS Loading = 0.1, $P_{reboiler}$ = 1.77 atm, $Z_{absorber}/Z_{base\ case}$ = 1, $Z_{stripper}/Z_{base\ case}$ = 1, Optimum L/G, Cooling at Absorber Middle

Relative Cooling Duty	L/G_{mass}	Lean Loading	Rich Loading	Q_{rel}
0.307	2.674	0.20	0.452	0.921

The solvent loop was not closed. It was kept open at the absorber inlet. In this way the lean solvent becomes an input to the model. Temperature, MEA concentration, and CO_2 loading of the stream are specified. The lean solvent rate is calculated with a design specification on the absorber block that keeps the removal at a specified value.

Sensitivity analyses were done on solvent rate, column heights, CO_2 removal, HSS loading, stripper pressure, and absorber temperature. The results of most runs are summarized in Table 2.

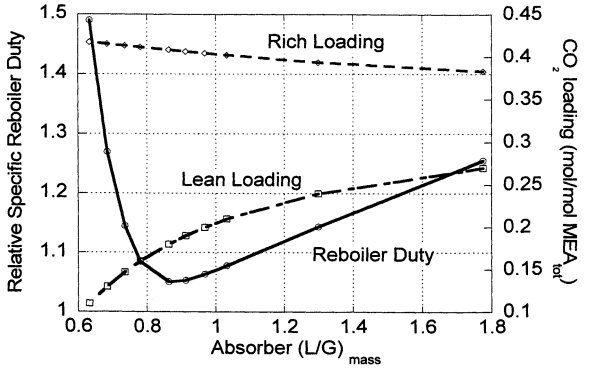

Figure 2. Optimization of solvent flow rate: 3% mole CO_2 in flue gas, 85% removal, 0.1 mol HSS/mol MEA_{tot}, solvent rate normalized to flue-gas rate.

Solvent rate

In order to optimize the solvent rate, the lean loading was varied and the solvent rate was calculated to keep the removal constant at 85%, with 3% CO_2 in the flue gas. Figure 2 demonstrates the optimum. At very low solvent rates, excessively low lean loading is necessary to maintain absorber performance. At the optimum solvent rate, the specified removal is achieved with a higher lean loading, which reduces the energy required to regenerate the solvent. At very high liquid rates, the energy required to heat the solvent to stripper temperature dominates the reboiler duty.

The heat provided in the reboiler by condensing steam is used in the stripper by three energy sinks: the heat of vaporization of water, the heat of desorption of CO_2, and the sensible heat to bring the solvent to reboiler temperature

$$Q_r = -n_{\mathrm{CO_2}}\Delta H_{abs,\mathrm{CO_2}} + \left(V - n_{\mathrm{H_2O}}\right)\Delta H_{\mathrm{vap,H_2O}} + Lc_p\left(T_{\mathrm{bottom}} - T_{\mathrm{top}}\right) \quad (13)$$

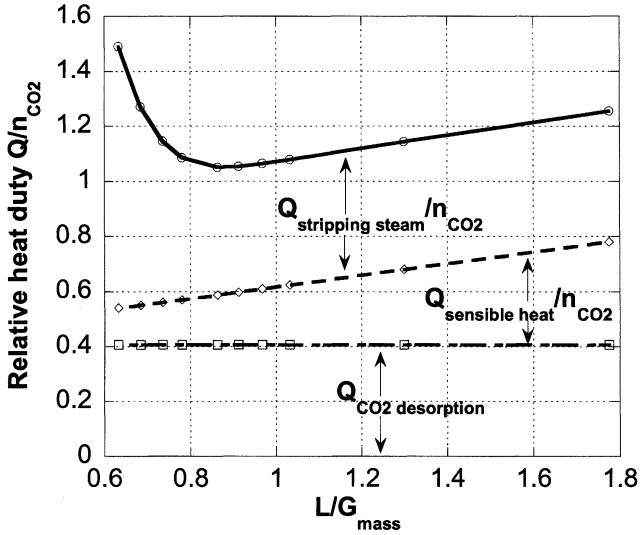

Figure 3. Allocation of the reboiler duty to CO_2 desorption, sensible heat, and stripping steam generation.

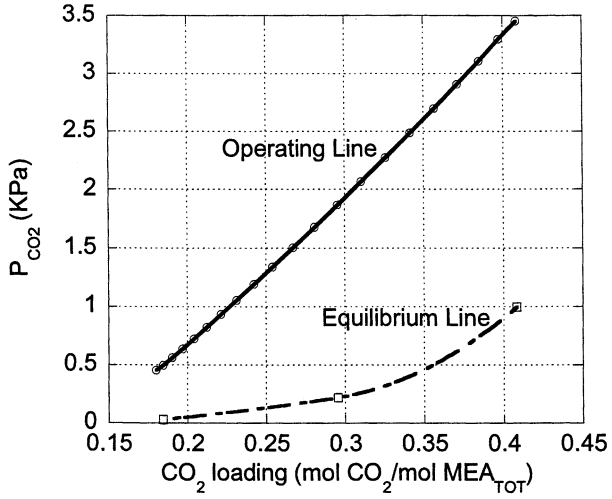

Figure 4. Absorber McCabe–Thiele diagram for optimum L/G case ($L/G_{\mathrm{mass}} = 0.86$): 3% CO_2 in flue gas, 85% removal, 33.5 wt % MEA, 0.1 mol HSS/mol MEA_{tot}.

Figure 3 shows the allocation of the reboiler duty to the three terms of Eq. 13. The RateFrac model uses rigorous estimates of these thermodynamic quantities. We have used approximations to develop Figure 3. Sensible heat was calculated assuming constant L and c_p in the stripper. At the average between stripper top and bottom conditions, ΔH_{abs} was assumed constant. Stripping steam was calculated by the difference between the calculated reboiler duty and the first two terms.

Sensible heat is linear, because it is directly proportional to L. Stripping steam is nonlinear and tends to an asymptote at high L/G. The relative energy requirement for CO_2 desorption is constant.

Optimum Case. Figures 4 and 5 show McCable–Thiele diagrams for absorber and stripper at the optimum solvent rate.

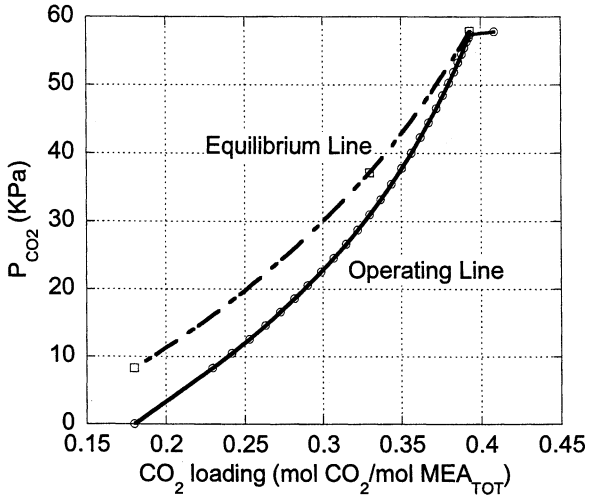

Figure 5. Stripper McCabe–Thiele diagram for optimum L/G case ($L/G_{\mathrm{mass}} = 0.86$): 3% CO_2 in flue gas, 85% removal, 33.5 wt % MEA, 0.1 mol HSS/mol MEA_{tot}.

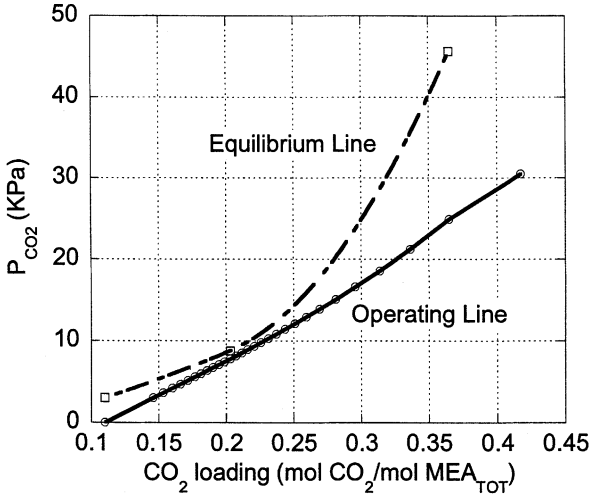

Figure 6. Stripper McCabe–Thiele diagram for low *L/G* case ($L/G_{mass} = 0.63$): 3% CO_2 in flue gas, 85% removal, 33.5 wt. % MEA, 0.1 mol HSS/mol MEA_{tot}.

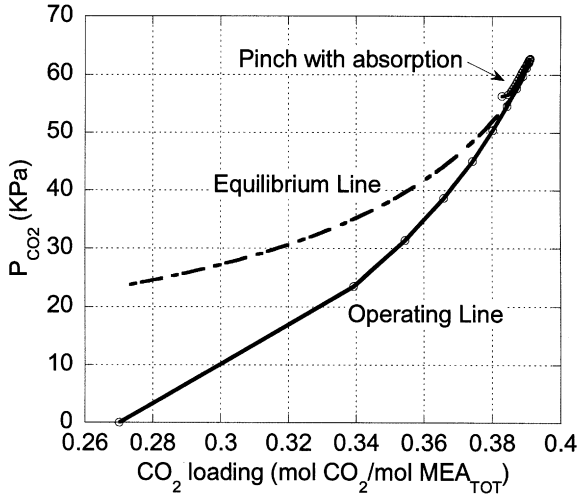

Figure 7. Stripper McCabe–Thiele diagram for high *L/G* case ($L/G_{mass} = 1.77$): 3% CO_2 in flue gas, 85% removal, 33.5 wt. % MEA, 0.1 mol HSS/mol MEA_{tot}.

The operating lines are obtained from the simulation. The circles drawn on them represent each RateFrac segment, with the same height of packing. For this sensitivity analysis, 20 segments were used to represent the absorber packing and 30 to represent the stripper packing. The equilibrium lines are obtained from flash calculations at the temperature and composition of three selected segments.

At the optimum solvent rate a rich pinch is observed in the stripper. Nevertheless, the separation is well distributed among the 30 segments. The rich pinch is a consequence of the nonlinear operating line. Water condenses from the vapor going up the column, thus curving the operating line toward the equilibrium line. The fact that the top of the stripper is approximately 10°C colder than the bottom reduces the nonlinearity of the equilibrium line, contributing to the formation of the rich pinch. A considerable separation is achieved in the reboiler stage, because it was modeled as an equilibrium segment.

At the rich end of the stripper there is a discontinuity in the loading at the feed stage. This is a consequence of flashing the hot feed to the lower equilibrium temperature at the top of the stripper.

The absorber McCabe–Thiele diagram shows that no equilibrium pinches are present, and a wide driving force is well distributed through all the segments, with a slightly higher concentration of segments at low loading, indicating that the optimum case is closer to a lean pinch rather than a rich pinch.

Low L/G. Figure 6 shows the stripper McCabe–Thiele diagram with a low solvent rate ($L/G_{mass} = 0.63$). The lean loading is low (0.11), in order to maintain the removal at 85% with the lower solvent rate. A tight pinch is observed in the middle of the stripper. The nonlinearity of the equilibrium relationship requires that the equilibrium be approached at an intermediate loading. Figure 3 shows that a large amount of stripping steam is required to overcome the middle pinch.

In the absorber there were no evident pinches, even though a rich pinch would be expected at low *L/G*.

High L/G. Figure 7 shows the McCabe–Thiele diagrams for the stripper at a high solvent rate. The stripper rich pinch is more definite, with more than half of the column working at the rich end, pinched conditions. From Figure 3, it can be seen that the stripping steam contribution to the heat requirement does not change significantly at high *L/G*. The sensible heat determines an increase in reboiler duty. The feed loading effect is reversed. Flashing is reduced, because of the lower rich loading. In this case, the loading increases at the top of the stripper, and it keeps increasing in the top half of the column. This is associated with CO_2 absorption in the top half of the column. The high liquid rate generates high liquid heat capacity; the vapor cannot heat up the liquid feed fast enough, and it gets cooled by it. Water condensation occurs, causing the CO_2 to become more concentrated in the vapor phase, to the point where absorption occurs.

There is no apparent equilibrium pinch in the absorber. However, half of the column is operating between 0.27 and 0.3 loading, suggesting a rate-based "pinch" at the lean end.

Effects of absorber height, CO_2 concentration, and CO_2 removal

The absorber height was varied about the value of the base case, with 3% CO_2/85% removal, 3% CO_2/90% removal, and 10% CO_2/90% removal (Figure 8). The absorber diameter and the stripper size were kept constant at the base-case value. The solvent rate was optimized for each case. The reboiler duty decreases with packing height, tending to an asymptote. The minimum duty was calculated increasing the height of the absorber at the point where the reboiler duty stopped changing. For the three curves, the values of the mimimum reboiler duties (relative to the reference arbitrary value) are 0.9425 (3% CO_2, 85% removal), 0.945 (3% CO_2, 90% removal), and 0.891 (10% CO_2, 90% removal). The minimum reboiler duty is practically independent of CO_2 removal.

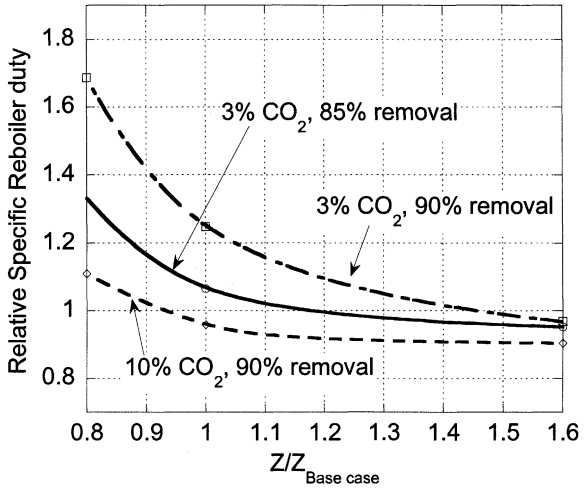

Figure 8. Effect of absorber height on reboiler duty per mole of CO_2 removed, 33.5 wt. % MEA, 0.1 mol HSS/mol MEA_{tot}, optimum solvent rate.

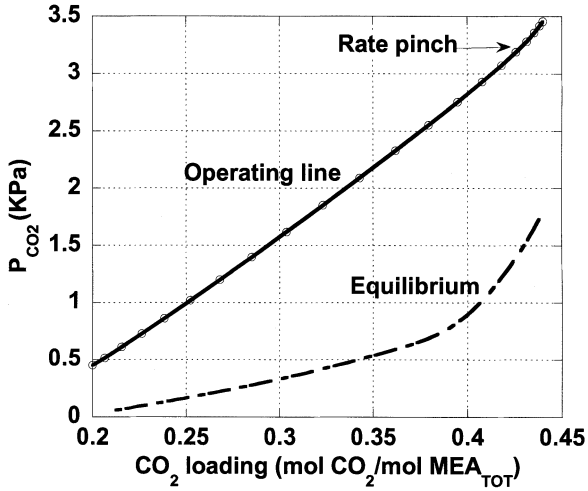

Figure 9. McCabe–Thiele diagram for the absorber: $Z_{absorber}/Z_{base\ case} = 1.6$, 33.5 wt % MEA, 0.1 mol HSS/mol MEA_{tot}, optimized solvent rate ($L/G_{mass} = 0.82$), 3 mol. % CO_2 in flue gas, 85% removal.

With a finite amount of packing, the reboiler duty increases with CO_2 removal, because the optimum solvent rate increases as the removal increases. This increases the sensible heat requirement.

At constant removal, the normalized reboiler duty increases as the CO_2 concentration in the flue gas decreases. Even though the absolute reboiler duty is higher for the 10% CO_2 case than the 3% CO_2 case, the reboiler duty normalized to the total number of moles recovered is lower. A simple explanation can be found if the minimum thermodynamic work required for the process is calculated at isothermal conditions (Eq. 14)

$$\frac{W_{\min}}{n_{CO_2}} = \Delta G_{T,P} = RT \ln \frac{P_{CO_2,\text{out}}}{P_{CO_2,\text{in}}} \tag{14}$$

For the case of 3 mol % of CO_2 in the flue gas, $P_{CO_2,\text{in}} = 0.03$ atm; for the 10% case, $P_{CO_2} = 0.1$ atm. Assuming an outlet pressure of 2 atm, the minimum work required to compress the CO_2 from the absorber inlet condition to the stripper outlet condition is $\ln(2/0.03)/\ln(2/0.1) = 1.4$ times higher in the low CO_2 case.

With 3% CO_2 and 85% removal at $z_{\text{absorber}}/z_{\text{base case}} = 1.6$, the reboiler duty is practically at its asymptotic value. A rich pinch would be expected in the absorber. Figure 9 shows the absorber McCabe–Thiele diagram for this case. The absorber does not appear to have an equilibrium pinch. However, the distribution of packing segments, represented by the circles on the operating line, shows that several segments achieve little change at the rich end. This apparent rate-based pinch is not determined by a low driving force. At the rich conditions there is a reduced concentration of free amine to enhance the reaction rates, therefore, the very low reaction rates reduce the rate of mass transfer.

Stripper height

The stripper height was varied to values less than the base case, for 3% CO_2 and 85% removal (Table 2c). In this analysis the liquid-phase mass-transfer performance in the stripper is overpredicted by the model, due to the use of instantaneous reactions. The stripper performance will also be overpredicted because the reboiler is modeled as an equilibrium segment.

The importance of the error introduced by using instantaneous reactions was estimated calculating gas and liquid mass-transfer resistances. The gas film resistance ranges from 50% to 70% in the base-case stripper. Since the reaction-rate resistance represents 20% to 70% of the liquid resistance (Freguia, 2002), 10% to 35% of the total mass-transfer resistance is neglected in the model.

The stripper height affects the heat requirement less dramatically than the absorber height. A column half as high could perform almost as well, with an increase in reboiler duty less than 4%.

This conclusion may be valid only for 3% CO_2. Figure 10 shows the McCabe–Thiele diagram for the stripper at 10% CO_2 at the optimum solvent rate. The stripper does not have an equilibrium pinch, as with 3% CO_2. This is because there is 3.3 times more CO_2 to transfer through the same gas–liquid contact area. Therefore, the stripper height should have a larger effect on reboiler duty with 10% CO_2.

Heat stable salts

The base case was calculated with HSS loading of 0.1 to represent probable effects of MEA degradation. The partial neutralization of MEA with a strong acid can increase the equilibrium partial pressure of CO_2 at a given temperature and loading, because strong acids shift the equilibrium toward the acid species CO_2. Figure 11 shows the McCabe–Thiele diagram for the stripper with no HSS and with 0.1 mol HSS/mol MEA_{tot}, at fixed solvent rate and lean loading. A reduction of 40% in the reboiler duty is obtained upon adding 10% HSS. With HSS loading = 0.1, the operating line follows the equilibrium line, keeping the driving force almost constant, typical of an optimized process. Without HSS, the re-

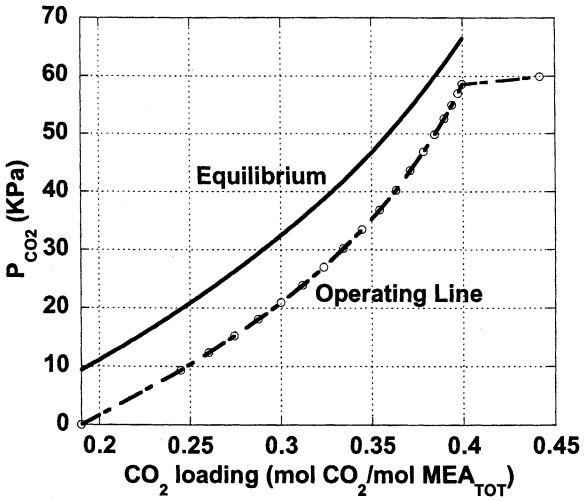

Figure 10. McCabe–Thiele diagram for the stripper: $Z_{absorber}/Z_{base\ case} = 1$, 33.5 wt % MEA, 0.1 mol HSS/mol MEA_{tot}, optimized solvent rate ($L/G_{mass} = 2.68$), 10 mol % CO_2 in flue gas, 90% removal.

boiler duty is 40% higher, because the solvent rate is not optimized. The addition of HSS changes the optimum solvent rate and the optimum lean loading.

The positive effects of HSS have been observed in other absorption/stripping systems with nonlinear equilibrium relationships (Kohl and Nielsen, 1997; Carey, 1990).

When the solvent rate is optimized, the effects of HSS are more limited. In Figure 12 the effect of HSS on reboiler duty is shown for three amine concentrations, with solvent rate optimized for each case. The effects on optimum lean loading and L/G are shown in Table 2d. The neutralization of 10% of the MEA reduces the reboiler duty by approximately 2%, whereas at nonoptimized conditions the reduction was 40%.

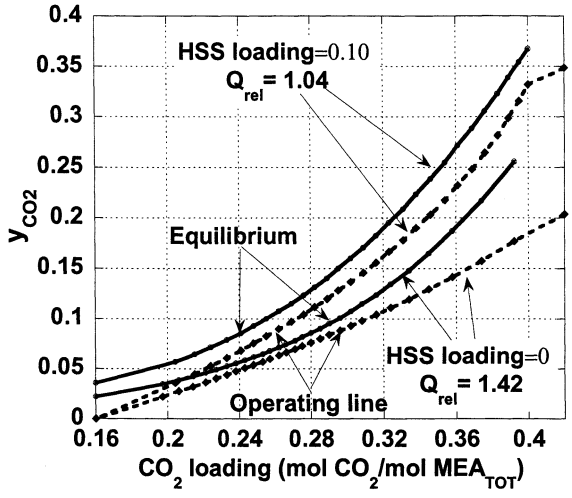

Figure 11. Comparison of base case Aspen Plus runs with 0 and 0.1 mol HSS/mol MEA_{tot}, heat-stable salts added on top of 30 wt. % active MEA: 3.13% CO_2 in flue gas, $L/G_{mass} = 0.78$.

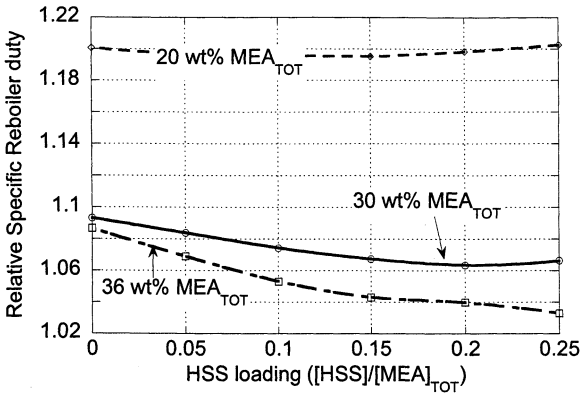

Figure 12. Effect of MEA concentration and of HSS loading on the reboiler duty, 3 mol % CO_2, 85% removal, optimum solvent rate.

Reboiler duty is reduced by increasing amine concentration, following Eq. 8. However, amine concentrations greater than 36% were not studied, because the diffusivity of CO_2 becomes so low that the absorption rates start to decrease, according to Eq. 8, and because MEA solvents become more corrosive when concentrated.

With 30 wt % MEA the minimum reboiler duty occurs at HSS loading of 0.2, indicating that HSS can slightly improve the performance of the process. Some HSS serves to linearize the equilibrium relationship and reduce steam requirement. However, at greater HSS, a high solvent rate is necessary, which increases reboiler duty because of sensible heat.

Effect of stripper pressure

Historically, stripper pressure has been designed for 1 to 2 atm to vent CO_2 and to minimize amine degradation, which can occur at a higher pressure/temperature (Rochelle et al., 2001). Because the ratio $P^*_{CO_2}/P^*_{H_2O}$ increases significantly with temperature, the reboiler heat duty will decrease with increased stripper pressure. However, in a thermally integrated power plant, it may be attractive to operate at lower pressure, because of the reduced cost of using lower pressure steam to drive the reboiler.

The effect of stripper pressure was analyzed at constant removal (85%) and CO_2 concentration in the flue gas (3%). The solvent rate was optimized, giving at $P = 0.5$ atm, $L/G_{mass} = 1.93$; and at $P = 3.7$ atm, $L/G_{mass} = 0.66$. Figure 13 gives the energy requirement for stripping as a function of the stripper pressure. Figure 14 gives the effect of pressure on the McCabe-Thiele diagram. The reboiler duty increases significantly at lower pressure, but only decreases slightly above 2 atm. The asymptote represents a minimum reboiler duty, when there is no stripping steam generated and the vapor is practically pure CO_2. The lost work of the reboiler steam was calculated with a Carnot efficiency, using a sink temperature of 40°C and a loss of 11°C for heat transfer across the reboiler. The work value of the reboiler steam has a minimum at about 1.5 atm, and only increases by approximately 30% at 0.5 atm. Therefore, the stripper can operate efficiently at any convenient level of steam pressure available from the power plant. The calculated lost work does not in-

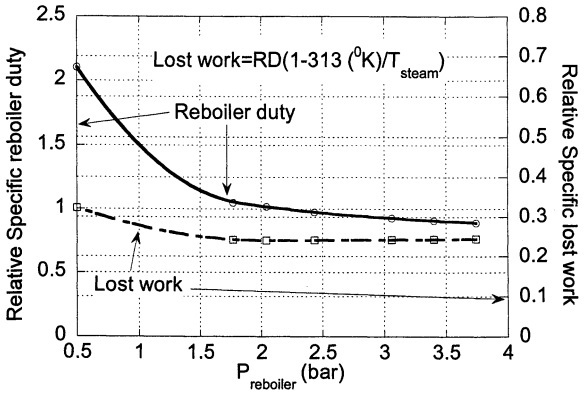

Figure 13. Effect of stripper pressure on the reboiler duty and lost work, for a 3 mol % CO_2 flue gas and 85% removal, 33.5 wt. % MEA, 0.1 mol HSS/mol MEA_{tot}, *L/G* optimized, 20°F approach in cross-exchanger.

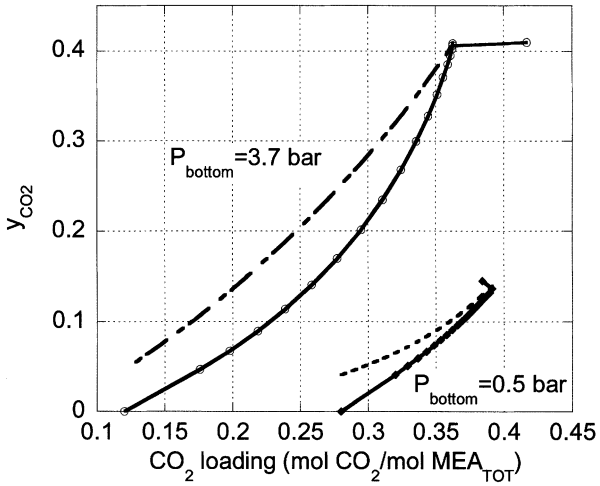

Figure 14. McCabe–Thiele diagrams for strippers operating at 3.7 and 0.5 bar, 3 mol % CO_2, 85% removal, 33.5 wt. % MEA, 0.1 mol HSS/mol MEA_{tot}, optimized *L/G*.

clude the additional compression cost for the CO_2, but that is small relative to the value of the reboiler steam. Table 2e presents more detailed results of this sensitivity analysis.

For a solvent with the ratio $-\Delta H_{abs,CO_2}/\Delta H_{vap,H_2O}$ equal to 1, the stripper pressure would not affect the reboiler duty. The stripper could be run at low pressure with lower-lost work. The compression cost would be part of the pressure optimization. Another advantage would be a lower amine degradation rate, due to lower operating temperature. Extensive work is underway to study solvents with a lower heat of absorption than MEA, such as piperazine-promoted K_2CO_3 (Cullinane, 2002).

Effect of intercooling

Figure 15 shows that the temperature in the middle of the absorber can be 15–35°C hotter than the temperature of the flue gas or solvent at either end. This phenomenon is caused by the heat of absorption of CO_2 and is more significant with 10% CO_2 than with 3% CO_2. The absorption rate of CO_2 can increase with temperature to the extent that the combined rate constant

$$\frac{\sqrt{k_2[\mathrm{MEA}]D_{CO_2}}}{H_{CO_2}}$$

increases with temperature. The rate of absorption will decrease to the extent that it is determined by the equilibrium driving force, $P_{CO_2} - P^*_{CO_2}$, which decreases with temperature.

Figure 15 shows that, for a 10% CO_2 absorber, the intercooling reduced the liquid temperature to 42°C in the middle of the absorber. Intercooling has practically no effect on the temperature in the rich end of the column. An amount of heat equal to one-third of the reboiler duty was removed from the liquid at the middle point of the absorber. The solvent rate was optimized and the removal was kept constant at 90%. However the reboiler duty was reduced only by 3.8%. Figure 16 compares the absorber McCabe–Thiele diagrams for the cooled and noncooled cases. The equilibrium line is lower for the cooled case, increasing the driving forces throughout the column, but only slightly improving the absorber performance.

Intercooling with 3% CO_2 in the flue gas will be less effective, because the temperature bulge is less significant.

Conclusions

With optimized solvent rate at the base-case conditions, the stripper approaches equilibrium at the rich end and has a well-distributed driving force throughout the rest of the con-

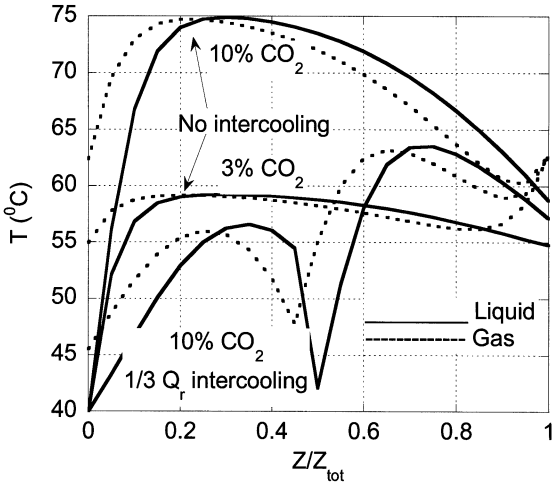

Figure 15. Comparison of liquid and gas temperature profiles for 10% CO_2–90% removal intercooled absorber, 10% CO_2–90% removal nonintercooled absorber, and 3% CO_2–85% removal nonintercooled absorber: intercooler at absorber middle point, cooling duty 1/3 reboiler duty, 0.1 mol HSS/mol MEA, optimized *L/G*.

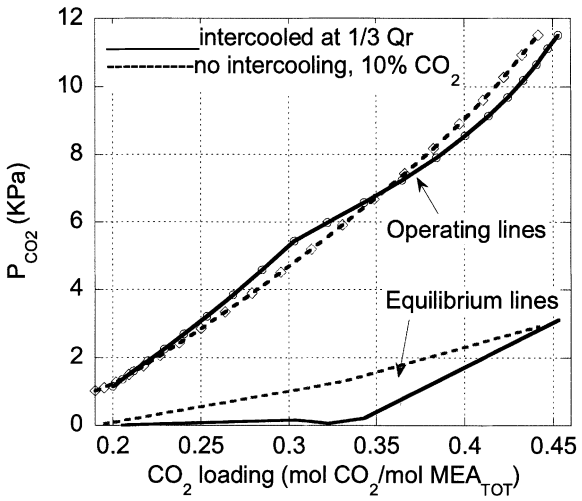

Figure 16. Comparison of absorber McCabe–Thiele diagrams for intercooled and nonintercooled absorber, intercooler at half column, intercooler duty 1/3 reboiler duty, 10% CO_2, 90% removal, 0.1 mol HSS/mol MEA, optimized *L/G*.

tactor. The rich pinch results from the decreased vapor rate at the top of the column. The absorber does not have a close approach to equilibrium, with high driving forces throughout the column.

The solvent circulation rate affects the steam requirements heavily, and can be optimized for each set of design conditions. A nonoptimized process can consume 50% more energy if the solvent rate is 30% smaller than the optimum, or 25% more if it is twice the optimum. The loss in performance is more important if the solvent rate is low, therefore, it is preferable to operate the process at a solvent rate slightly higher than the optimum. All of the following conclusions assume an optimized solvent rate.

Steam consumption is reduced by a greater height of packing in the absorber. By providing more area for mass transfer, it is possible to enhance the process performance. The effect is important with less packing, whereas with a large amount of packing the effect disappears and the reboiler duty reaches an asymptote, only 10% less than the base-case design. Even with a considerable height of packing, the absorber does not approach equilibrium. In reality, at the rich end many stages achieve very little removal. The "pinch" is determined by slow kinetics, rather than low driving forces.

Steam consumption is only reduced slightly by increased packing height in the stripper, at the base-case conditions of this study. The stripper height required is much less than that of the absorber, because, due to higher temperature, the reaction rate is not limiting. The amount of packing in the stripper should be scaled according to the amount of CO_2 removed.

An increase in CO_2 content in the flue gas and the reduction of CO_2 removal are accompanied by a small reduction in the specific steam consumption (kJ/mol CO_2). The effects tend to disappear if the columns are oversized.

The addition of a strong acid to the solvent forms HSS, which can slightly reduce the energy requirement, by making the equilibrium relationship more linear. At a constant solvent rate, the addition of HSS can change steam consumption by as much as 40%.

The stripper pressure affects the ratio of CO_2:H_2O in the stripper vapors, affecting the reboiler duty and the lost work. An optimum pressure is found at approximately 1.5–2 atm. The effect is not very significant, therefore, it is possible to operate at any convenient pressure.

Intercooling increases absorption rates in the absorber, by increasing the driving force for absorption. The effect is moderate, since a heat stream equal to one-third of the reboiler duty reduces the latter by only 4%, when extracted from the center of the absorber.

Acknowledgments

The authors acknowledge the financial support from Fluor Daniel, Inc., and from the Texas Advanced Technology Program. The authors are grateful to Carl Mariz at Fluor Daniel for the important field information provided, and to Venkat Venkataraman at Aspen Technology for the help provided in creating the RateFrac kinetic subroutine.

Notation

$a_{CO_2,i}$ = activity of CO_2 at the gas–liquid interface
$a_{CO_2^*i}$ = activity of CO_2 in equilibrium with the interface composition
C_{tot} = total concentration of liquid phase, M
D = column diameter, m
D_{CO_2} = diffusivity of CO_2 in solution, m^2/s
$D_{CO_2,water}$ = diffusivity of CO_2 in water, m^2/s
HSS loading = heat stable salts loading
G = gas flow rate in absorber, kmol/s
$\Delta H_{abs,CO_2}$ = heat of absorption, kJ/mol
$\Delta H_{vap,H_2O}$ = heat of vaporization of H_2O, kJ/mol
H_{CO_2} = Henry's constant of CO_2, atm/M
$[j]_i$ = concentration of species j at the interface, $kmol/m^3$
k_2 = rate constant of second-order reactions, m^3/kmol s
K = equilibrium constant
L = liquid flow, kmol/s
N_{CO_2} = flux of CO_2, $kmol/m^2s$
n_{CO_2} = moles of CO_2 removed from flue gas, kmol/s
P = total pressure, atm
Q_r = reboiler duty, MJ
Q_{rel} = relative reboiler duty, dimensionless
R = reaction rate, M/s
R = universal gas constant, 8.314 kJ/kmol K
T = temperature, K
V = vapor flow rate in stripper, kmol/s
x_j = liquid mole fraction of species j
y_j = gas mole fraction of species j
Z = height of packing in a column, m

Greek letters

α = CO_2 loading
γ_j = activity coefficient of species j with reference state at pure component
$\mu_{solution}$ = viscosity of solution
μ_{water} = viscosity of water

Literature Cited

Al-Baghli, N. A., S. A. Pruess, V. F. Yesavage, and M. S. Selim, "A Rate-Based Model for the Design of Gas Absorbers for the Removal of CO_2 and H_2S Using Aqueous Solutions of MEA and DEA," *Fluid Phase Equilib.*, **185**, 31 (2001).

Austgen, D. M., *A Model for Vapor-Liquid Equilibrium for Acid Gas-Alkanolamine-Water Systems*, PhD Diss., The Univ. of Texas at Austin (1989).

Austgen, D. M., G. T. Rochelle, and C. C. Chen, "A Model for Vapor-Liquid Equilibria for Aqueous Acid Gas-Alkanolamine Systems Using the Electrolyte-NRTL Equation," *Ind. Eng. Chem. Res.*, **28**, 1060 (1989).

Carey, T. R., *Rate-Based Modeling of Acid Gas Absorption and Stripping Using Aqueous Alkanolamine Solutions*, MS Thesis, The Univ. of Texas at Austin (1990).

Chen, C. C., H. I. Britt, J. F. Boston, and L. B. Evans, "Extension and Application of the Pitzer Equation for Vapor-Liquid Equilibrium for Aqueous Electrolyte Systems with Molecular Solutes," *AIChE J.*, **25**, 820 (1979).

Cullinane, J. T., *Carbon Dioxide Absorption in Aqueous Mixtures of Potassium Carbonate and Piperazine*, MS Thesis, The Univ. of Texas at Austin (2002).

Dang, H., *CO_2 Absorption Rate and Solubility in Monoethanolamine/Piperazine/Water*, MS Thesis, The Univ. of Texas at Austin (2001).

Freguia, S., *Modeling of CO_2 Removal from Flue Gases with Monoethanolamine*, MS Thesis, The Univ. of Texas at Austin (2002).

Hikita, H., S. Asai, H. Ishikawa, and M. Honda, "The Kinetics of Reactions of Carbon Dioxide with Monoethanolamine, Diethanolamine and Triethanolamine by a Rapid Mixing Method," *Chem. Eng. J.*, **13**, 7 (1977).

Holmes, J. W., M. L. Spears, and J. A. Bullin, "Sweetening LPG's with Amines," *Chem. Eng. Prog.*, **80**(5), 47 (1984).

IEA Greenhouse R&D Programme. www.ieagreen.org.uk/reports.htm, accessed 5/23/2002.

Jou, F. Y., A. E. Mather, and F. D. Otto, "The Solubility of CO_2 in a 30 Mass Percent Monoethanolamine Solution," *Can. J. Chem. Eng.*, **73**, 140 (1995).

Kohl, A. L., and R. B. Nielsen, *Gas Purification*, 5th ed., Houston, TX (1997).

Lee, J. I., F. D. Otto, and A. E. Mather, "Equilibrium Between Carbon Dioxide and Aqueous Monoethanolamine Solutions," *Appl. Chem. Biotechnol.*, **26**, 541 (1976).

Liljedahl, G., J. Marion, and D. Vogel, "Technical and Economic Feasibility of CO_2 Capture on an Existing U.S. Coal-Fired Power Plant," Int. Joint Power Generation Conf., New Orleans, LA (2001).

Mock, B., L. B. Evans, and C. C. Chen, "Thermodynamic Representation of Phase Equilibria of Mixed-Solvent Electrolyte Systems," *AIChE J.*, **32**(10), 1655 (1986).

Pacheco, M. A., *Mass Transfer, Kinetics and Rate-Based Modeling of Reactive Absorption*, PhD Diss., The Univ. of Texas at Austin (1998).

Pinsent, B. R. W., L. Pearson, and F. J. W. Roughton, "The Kinetics of Combination of CO_2 with NH_3," *Trans. Faraday Soc.*, **52**, 1594 (1956).

Rochelle, G. T., S. Bishnoi, S. Chi, and H. Dang, "Research Needs for CO_2 Capture from Flue Gas by Aqueous Absorption/Stripping," Final report, U.S. Dept. of Energy, Federal Energy Technology Center, Washington, DC (2001).

Sherwood, T. K., R. L. Pigford, and C. R. Wilke, *Mass Transfer*, McGraw-Hill, New York (1975).

Weiland, R. H., and J. C. Dingman, "Column Design Using Mass Transfer Rate Simulation," *Proc. Annu. Conv.*—Gas Processor Assoc., Optimized Gas Treating, Inc., Houston, TX, p. 80 (2001).

Weiland, R. H., "Physical Properties of MEA, DEA, MDEA and MDEA-Based Blends Loaded with CO_2," GRI/GPA Research Report RR-152, Gas Processors Association, Tulsa, OK (1996).

Zhang, D. D., and H. J. Ng, "Modeling of Liquid Hydrocarbon Sweetening with Amine Solutions," *Proc. Annu. Conv.—Gas Process. Assoc.*, Denver, CO, p. 22 (1996).

Manuscript received Sept. 9, 2002, and revision received Jan. 28, 2003.